Published in final edited form as:
Cancer Res. 2013 June 15; 73(12): 3555–3565. doi:10.1158/0008-5472.CAN-12-2845.

A novel model for evaluating therapies targeting human tumor vasculature and human cancer stem-like cells

Daniela Burgos-Ojeda[1], **Karen McLean**[2], **Shoumei Bai**[1], **Heather Pulaski**[2], **Yusong Gong**[3], **Ines Silva**[3], **Karl Skorecki**[4], **Maty Tzukerman**[4], and **Ronald J. Buckanovich**[1,2,3]

[1]Cell and Molecular Biology Program, University of Michigan, Ann Arbor, MI

[2]Department of Obstetrics and Gynecology, Division of Gynecologic Oncology, University of Michigan, Ann Arbor, MI

[3]Department of Internal Medicine, Division Hematology-Oncology, University of Michigan, Ann Arbor, MI

[4]Rambam Medical Center and Sohnis-Forman Stem Cell Center at the Technion-Israel Institute of Technology, Haifa Israel

Abstract

Human tumor vessels express tumor vascular markers (TVMs), proteins that are not expressed in normal blood vessels. Antibodies targeting TVMs could act as potent therapeutics. Unfortunately, preclinical in vivo studies testing anti-human TVM therapies have been difficult to perform due to a lack of in vivo models with confirmed expression of human TVMs. We therefore evaluated TVM expression in a human embryonic stem cell derived teratoma (hESCT) tumor model previously shown to have human vessels. We now report that, in the presence of tumor cells, hESCT tumor vessels express human TVMs. The addition of mouse embryonic fibroblasts and human tumor endothelial cells significantly increases the number of human tumor vessels. TVM induction is mostly tumor type specific with ovarian cancer cells inducing primarily ovarian TVMs while breast cancer cells induce breast cancer specific TVMs. We demonstrate the utility of this model to test an anti-human specific TVM immunotherapeutics; anti-human Thy-1 TVM immunotherapy results in central tumor necrosis and a three-fold reduction in human tumor vascular density. Finally, we tested the ability of the hESCT model, with human tumor vascular niche, to enhance the engraftment rate of primary human ovarian cancer stem-like cells (CSC). $ALDH^+$ CSC from patients (n=6) engrafted in hESCT within 4–12 weeks whereas none engrafted in the flank. ALDH- ovarian cancer cells showed no engraftment in the hESCT or flank (n=3). Thus this model represents a useful tool to test anti-human TVM therapy and evaluate in vivo human CSC tumor biology.

Keywords

Tumor Vasculature; Cancer Stem Cells; Immunotherapy; Human Embryonic Stem Cells

INTRODUCTION

The tumor vasculature expresses numerous genes not expressed in normal vasculature (1–5). This is in part due to the increased expression of genes associated with physiologic

Contact: Ronald J. Buckanovich, MD, PhD, Rm 5219 Cancer Center, 1500 E. Medical Center Drive, Ann Arbor, MI 48109, ronaldbu@med.umich.edu, Phone (734)-764-2395, Fax (734)-936-7376.

Disclosure of potential conflicts of interest: The authors have no conflicts of interest to report

angiogenesis, as many tumor vascular antigens are also upregulated in angiogenic tissues (1, 6, 7). However, if the angiogenic signature is the primary difference between tumor vasculature and normal vasculature, one might anticipate a significant overlap between vascular profiles of different tumor types. Indeed this is not the case; the vascular expression profile of different tumor types appears to be distinct (3, 5, 7–10). This is consistent with murine studies suggesting physiologic and pathologic angiogenesis have distinct gene signatures (6), and indicates that the influence of the cancer cell on the tumor microenvironment may play a role in the induction of tumor specific vascular proteins.

Tumor vascular markers (TVMs), antigens specifically expressed in tumor vessels and not expressed in normal vessels, represent a potentially important therapeutic target. In particular, those with extracellular exposure are ideal targets for immunotherapeutics (2, 10–12). As therapeutic targets, TVMs would be accessible to drug, and the restricted nature of TVM expression should limit therapy-associated side effects on normal tissues. Proof-of-principle studies in rodents demonstrated the potency of tumor vascular targeted therapy. Immunotherapeutics targeting a tumor vascular specific splice variant of fibronectin demonstrated profound restriction of tumor growth (13). More recently, antibodies targeting the anthrax receptor (Tem8) have been shown to specifically inhibit pathologic angiogenesis, and restrict tumor growth (14, 15). Phase I clinical trials using an immunotherapeutic targeting the TVM FOLH1 suggest anti-tumor vascular immunotherapeutics are safe and potentially efficacious (16).

Broader development of anti-TVM therapies has been hindered by the absence of an experimental system with confirmed human TVM expression with which to test potential therapies. Most mouse tumor models generate murine vessels and therefore cannot be used to test antibodies specific to human antigens. While models of human tumor vasculature have been proposed, these models have been difficult to reproduce, have limited long term viability, and/or do not have confirmed expression of TVMs (17–19).

Beyond their role in providing nutrients to the tumor, tumor vascular cells are also a critical host component of the cancer stem-like cell (CSC) niche. Vascular cells receive angiogenic cues from CSC and in turn provide CSC with critical survival, proliferation, and differentiation signals (20). Thus a model with robust human tumor vasculature could enhance the in vivo study of human CSC, which have been surprisingly difficult to engraft in mice. The difficulty engrafting human CSC in mice could be related to differences in the murine and human microenvironments, including the vasculature.

In the current study we focused on detailed characterization of the vasculature using the previously reported human embryonic stem cell teratoma (hESCT) tumor model previously demonstrated to have human vessels (21, 22). This model has the ease of standard xenograft models, however tumor vessels are derived from the human ESC and are therefore of human origin. It had not been clear if these are ‘normal’ human vessels or true ‘tumor vessels’ that express TVMs. Here, we demonstrate that, when injected with cancer cells, hESCT have vessels expressing human TVMs. With the addition of mouse embryonic fibroblasts and primary tumor vascular cells, ~80% of the vessels in the tumor are human in origin and persist for up to 12 weeks. Using hESCT ovarian cancer and breast cancer models, we found that several TVMs are induced in a tumor specific fashion. We then used this model to demonstrate the ability to test the therapeutic activity of anti-human tumor vascular specific antibody therapeutics; an anti-THY1 immunotoxin delayed tumor growth and resulted in central tumor necrosis. Finally, we demonstrated that this tumor model, with a human microenvironment, enhances the engraftment and growth of primary ovarian CSC.

MATERIALS AND METHODS

Cell Culture

Use of hESC was approved by the University of Michigan Embryonic Stem Cell Research Oversight Committee. H9 hESC (WiCell Research Institute, Madison, WI) and H7-GFP hESC (a gift from Joseph Wu, Stanford University) were grown as previously described (23). Undifferentiated ESC colonies were initially passaged by manual dissection with final passages performed with enzymatic digestion using TrypLE Select (Invitrogen, Carlsbad, CA). Human ovarian cancer cell line HEY1 and SKOV3 (American Type Culture Collection, Manassas, VA) were grown in RPMI containing 10% FBS. The breast cancer cell line MCF7 (a gift from Dr. Max Wicha, University of Michigan) was grown in MEM containing 10% FBS and 0.01 mg/ml bovine insulin (Invitrogen, Carlsbad, CA). In order to create DsRED expressing cells, both MCF7 and HEY1 cells were transduced with DsRED expressing lentiviral construct (provided by the UMCC Vector core).

In vivo Tumor Models

NOD/SCID mice (Charles River, Wilmington, MA), were housed and maintained in the University of Michigan Unit for Laboratory Animal Medicine. All studies were approved by the University Committee on the Use and Care of Animals. hESCT were generated as previously described (21–23). Briefly, H9 hESC were cultured on mouse embryonic fibroblasts (MEFs), manually dispersed and passaged. Approximately 5×10^5 undifferentiated H9 hESC or H7-GFP ESC were injected subcutaneously into the axilla of NOD/SCID mice (with or without MEFs) with 100 μl of PBS and 200 μl of matrigel (BD Biosciences, San Diego, CA). Once hESCT were palpable, tumor cells in 40 μl of PBS were injected intra-hESCT. 2×10^5 tumor cells (HEY1-DsREd or MCF7 DsRED) were injected alone or with 5,000 VE-Cadherin$^+$ primary human tumor vascular cells (isolated as previously described) (7). For hESCT injected with primary ovarian CSCs, 700 (n=2), 5000 (n=3), or 10,000 (n=3) primary ALDH$^+$ ovarian cancer cells (from 6 different patients) or 10,000 ALDH$^-$ cells from paired samples were injected (n=3). All tumor were harvested when hESCT-tumor volumes were ~2000 mm^3 (range 4–12 weeks, median 8 weeks). For flank xenografts, 5×10^5 cells were injected in 100 μl of PBS and 200 μl of matrigel into the axilla of NOD/SCID mice. Tumors were imaged using bio-fluorescence (Xenogen IVIS 2000, Caliper Life Sciences, Hopkinton, MA. Murine tumors were APC/PTEN/p53 mutant mouse ovarian tumors (a gift from Dr. Kathy Cho, University of Michigan) (24, 25).

Isolation of Cancer Stem Cells from Primary Ovarian Cancer Specimens

Informed written consent was obtained from all patients before tissue procurement. All studies were performed with the approval of the Institutional Review Board of the University of Michigan. All tumors were from patients with stage III or IV epithelial ovarian or primary peritoneal cancer. Tumors were mechanically dissected into single-cell suspensions, red cells lysed with ACK buffer, and cell pellets were collected by centrifugation. CSC were then isolated from primary ovarian tumor single cell suspensions using the ALDEFLUOR assay fluorescence activated cell sorting (FACS) as previously described (26). Gating was established using propidium iodide (PI) exclusion for viability. ALDH/DEAB treated cells were used to define negative gates. FACS was performed using the BD FACSCanto II or FACSAria (Becton Dickinson) under low pressure in the absence of UV light.

Immunofluorescence (IF) and Immunohistochemistry (IHC)

8 μm sections from fresh frozen tumors were fixed in acetone for 10 min and then washed with PBS and blocked for 20 min. Primary antibody was incubated for 2 hr, washed with

PBS and incubated with secondary antibody for 1 hr. For IF, slides were washed with PBS and then mounted with Vectashield Mounting Medium for fluorescence with DAPI H-1200 (Vector Laboratories, Burlingame, CA). Antibodies used for IF and IHC are listed in Supplementary Table 1. IHC staining was performed using the Vectastain ABC kit (Vector, Burlingame, CA) per manufacturer's instructions. Select p53 IHC was performed by the Histology/IHC Service at the University of Michigan.

RNA Isolation and RT-PCR

Tumors were sectioned and regions of tumor with human vasculature were confirmed via IHC. Serial sections of were dissolved in Trizol (Invitrogen, Carlsbad, CA) and RNA was extracted (PureLink RNA Mini Kit, Invitrogen, Carlsbad, CA) per manufacturer recommendations. RNA integrity was confirmed on the Agilent 2100 BioAnalyzer. PCR was performed for 40 cycles with primers at 100 nM concentrations (Supplementary Table 2). All transcripts were confirmed using 3% agarose gel electrophoresis.

Quantification of Vessels

Vascular density quantification was performed as previously described (27). Five sections from each of three tumors in each tumor group were evaluated. Total mCD31 and hCD31 stain, as defined by pixel density and hue, was assessed using Olympus Microsuite Biological Suite Software. The area of staining was then compared between mCD31 and hCD31 using a two-sided student t-test. $hCD31^+$ tumor microvascular density following anti-THY1-toxin therapy were similarly assessed. hCD31-PE and Alexa 594 Goat anti-GFP were used to assess human vessels either from tumor endothelial cell origin (PE^+ only) or from hESCT origin (PE^+ and GFP^+). Sections were photographed in toto, and then quantitated using Olympus software as above.

Immunotoxin Development and Delivery

Anti-THY1-saporin immunotoxin was developed as previously described (27). 2 μg of freshly conjugated anti-THY1 antibody and saporin toxin, or an equimolar concentration of strepavidin-saporin, or unlabeled anti-THY1 antibody was incubated with 5×10^4 mesenchymal stem cells (MSC) in triplicate. After three days of treatment, viability cell was assessed using Trypan Blue. To test the efficacy of anti-TVM therapeutics in vivo hESCT-HEY1 tumors were treated with no treatment (n=3), or 2 μg of rat IgG-saporin (n=3), or anti-THY1-saporin (n=4). Immunotoxin was delivered intravenously every other day for 3 doses. Tumor growth was tracked using biofluorescent imaging with the Xenogen IVIS 200 imaging system and LivingImage software provided by the Center of Molecular Imaging of the University of Michigan. Mice were monitored the day before and after treatment. This experiment was repeated with rat IgG-saporin controls (n=3) and anti-Thy-1-saporin (n=3).

RESULTS

Vessels in hESCT-Cancer Model Express TVMs in a Cancer Cell Dependent Manner

We generated hESCT-ovarian cancers (HEY1) and hESCT-breast cancers (MCF7) as previously described (23) using DsRED labeled cancer cells. Immunofluorescence demonstrated clear, non-DsRED, human $CD31^+$ vessels consistent with prior reports of human ESC derived vessels (21, 22, 28, 29). Human vessels were predominantly found in a peri-tumoral location (Fig 1A), and less frequently within the tumor islets and teratoma tissue. RT-PCR was performed to determine if the ovarian or breast specific TVMs were expressed in (1) HEY1 ovarian cancer cell culture, (2) HEY1 ovarian tumor xenografts, (3) in vivo hESCT, or (4) in vivo hESCT- HEY1 ovarian tumors. In parallel we assessed the expression of ovarian or breast cancer specific TVMs were expressed in (1) MCF7 ovarian

cancer cell culture, (2) MCF7 breast cancer xenografts, (3) in vivo hESCT, or (4) in vivo hESCT-MCF7 breast tumors. We evaluated the expression of TVMs that have been reported to be upregulated in numerous tumors, including tumor endothelial marker-7 (TEM7), Integrin β3, and THY1, as well as for TVMs reported to be ovarian cancer specific including EGFL6, P2Y-like receptor (GPR105), and F2RL1, or breast cancer specific such as FAP, HOXB2, SFRP2, and SLITRTK6. Unfortunately all TVM mRNAs (and every gene we have tested to date) were expressed in both hESCT and the ovarian cancer and breast cancer hESCT-cancer model, thus RT-PCR suggested TVMs were expressed in the hESCT but was otherwise uninformative (Fig 1B).

We next performed immunohistochemistry (IHC) to localize TVM expression within the cell line xenografts, hESCT, hESCT-HEY1 ovarian tumors, and hESCT-MCF7 breast cancers. Within hESCT controls, TVM protein expression could be identified in various developmental tissues, but expression was generally not found in vascular structures (Fig 2). In contrast, the expression of ovarian TVMs could be detected within peri-tumoral vessels within the hESCT-HEY1 ovarian tumors (Fig 2). Some vessels were clearly filled with red blood cells, indicating a connection with the murine vasculature and perfusion (Fig 2 and data not shown). Serial sections stained with anti-hCD31 antibody confirmed these structures as human vessels (Sup. Fig S1). Identical results were obtained in a hESCT-SKOV3 ovarian cancer model (data not shown). Similarly, the breast cancer specific TVMs FAP, SFRP2, SLITRK6, and SMPD3, were all expressed in the hESCT-MCF7 tumors (Fig 2). No vascular expression of any of the TVMs was detected in flank tumor xenografts (Fig 2) or in a murine ovarian tumor model (Supplemental Fig 2), demonstrating the IHC is not detecting murine tumor vessels.

It remained unclear if the distinctions in the tumor vascular expression profile observed for different tumors is related to different methodologies of TVM identification, or a true distinction in the pattern of expression related to the tumor specific microenvironment. We therefore also assessed the vascular expression of ‘breast’ TVMs in the hESCT-HEY1 ovarian cancer model and the expression of ‘ovarian’ TVMs within the hESCT-MCF7 breast cancer model. Interestingly vascular expression of the ‘ovarian’ TVMs F2RL1, GPR105 and EGFL6 was not detected in the hESCT-MCF7 breast cancer model (Fig 2). Similarly the ‘breast’ TVMs FAP and SFRP2 were not expressed in the vasculature of the hESCT-HEY1 ovarian tumors (Fig 2). Rare vascular expression of the ‘breast’ TVMs SLITRK6 and SMPD3 was detected in the hESCT-HEY1 ovarian tumor model (Fig 2). These findings suggest that some TVMs are expressed in a cancer specific manner and therefore likely induced by tumor cells, while others are more promiscuous and may identify angiogenic vessels or vasculogenesis.

Enhancing Human Vascular Density in the hESCT Cancer Model

A primary goal of this study was to determine if this model could be used to test anti-human TVM immunotherapeutics. However, initial studies demonstrated that only a minority of resultant vessels (~15%) were of human origin with the remainder being murine vessels (see below). In order to increase the utility of the model for testing anti-vascular therapeutics, we attempted to increase the percentage of human tumor vessels in the hESCT-cancer model. As fibroblasts in the ovarian tumor microenvironment can significantly promote angiogenesis (31), we co-injected hESC and irradiated mouse embryonic fibroblasts (MEFs) to create a hESCT in which to inject HEY1 ovarian cancer cells. Alternatively hESCT +MEFs we co-injected with HEY1 ovarian cancer cells and 5,000 FACS isolated VE-Cadherin^{+} primary ovarian tumor endothelial cells. Human CD31 IHC demonstrated the greatest number of human vessels in tumors co-injected with MEFs and VE-Cadherin^{+} cells (Fig 3A). Interestingly, while there were regions of the tumor, which had overlapping and interconnected human and murine vessels (Fig 3B), most regions of the tumor were

dominated by either human or murine vessels (data not shown). IHC analysis of these vessels confirmed the expression of TVMs (data not shown). Quantification of the vascular density of murine and human vessels using co-IF with human CD31 and murine CD31 revealed that while the hESCT-HEY1 ovarian cancer tumor model alone had ~15% human vessels, the addition of MEFs increased the percentage of human vessels to ~40% (p value of 0.01, Fig 3C). With the addition of VE-Cadherin^{+} tumor endothelial cells nearly 80% of the tumor vessels were human (p value <0.0001, Fig 3C). HEY1 cells co-injected with 5000 VE-Cadherin^{+} cells in matrigel in the animals flank, demonstrated no human vessels (data not shown) demonstrating the profound human vascularity is unique to the hESCT model. In order to determine if the increase in human vessels in the presence of VE-Cadherin^{+} cells was due to increased angiogenesis from the hESCT cells or proliferation of the VE-Cadherin^{+} cells, we repeated the above experiment using GFP labeled H7 ESC (Fig 3D). Evaluation of tumor vessels demonstrated that 60–80% of the human vessels were GFP$^{(-)}$ and thus derived from the ovarian cancer VE-Cadherin^{+} cells while the remaining 20–40% of human vessels were GFP^{+} and therefore derived from hESCT cells (Fig 3E). These data demonstrate that the addition of human tumor vascular cells to this model leads to a dramatic increase in human tumor vasculature such that the majority of vessels present in the tumor are human in origin.

Testing an Anti-TVM Therapeutic in the hESCT-Ovarian Cancer Model

In order to test the utility of this model for screening anti-human TVM immunotherapeutics, we developed an immunotoxin targeting the human TVM THY1. This antigen was chosen due to the availability of commercial antibodies that can recognize the THY1 antigen in vivo. In order to create the immunotoxin, streptavidin-conjugated saporin toxin was coupled to a biotinylated anti-human THY1 antibody. The cytotoxicity of this immunotoxin was confirmed in vitro against THY1^{+} primary human mesenchymal stem cells (MSC); anti-THY1-immunotoxin resulted in statistically significant MSC death relative to antibody alone or saporin toxin alone controls (Fig 4A). In order to test the efficacy of anti-TVM-immunotoxin in vivo, anti-THY1-saporin (n=7 total in two experiments) immunotoxin or control rat IgG-saporin (n=6 total in two experiments) was delivered intravenously to mice bearing hESCT-HEY1 DsRed tumors. Tumor growth was tracked with biofluorescent imaging. While rat IgG-saporin treated tumors demonstrated continued growth, THY1-Saporin treated hESCT-HEY1 ovarian tumors demonstrated delayed growth and significant reduction in central tumor viability (the region dependent on human vessels) (Fig 4B-C). Following completion of therapy, growth resumed in peripheral tumor regions that were dependent on murine vessels continued to expand (Fig 4B and data not shown). Control hESCT alone and HEY1-DsRED flank tumors showed no response to either therapy (data not shown).

To further analyze the impact of anti-THY1 therapy on the human vessels, we quantified human tumor microvascular density using anti-hCD31 IHC. There was a three-fold reduction in the number of human vessels in hESCT-HEY1 ovarian tumors treated with anti-THY1 saporin toxin compared with Rat IgG-saporin toxin treated controls (Fig 4D). These results confirm the utility of this model for testing human TVMs specific therapeutics in vivo.

The hESCT Model Promotes the in vivo Growth of Primary Human Cancer Stem Cells

Human ovarian CSC have been particularly challenging to grow in vivo. Engraftment rates of CSC directly isolated from human ovarian tumors are only 20–40% in traditional flank tumor models and 5,000 CSC typically require 6–12 months to create a tumor (26). We hypothesized that the human microenvironment of the hESCT model with a human tumor vascular niche could greatly enhance the growth of ovarian CSC. Using ALDH as an

ovarian CSC marker (26), we assessed the efficiency of primary human ovarian CSC engraftment in the hESCT tumor model. We injected FACS isolated $ALDH^+$ primary human ovarian CSC (700–10,000) from 6 ovarian cancer patient samples into either hESCT or subcutaneously. hESCT were allowed to grow until they reached ~2000 mm^3 (4–12 weeks after tumor cell injection). Histochemical analysis of resected hESCT-$ALDH^+$ CSC demonstrated regions consistent with papillary serous tumor growth (Fig 5A and data not shown). In order to confirm these areas represent ovarian tumor cells, we exploited the recent finding that p53 is mutant in >95% of serous ovarian tumors (30). p53 IHC clearly identified human $p53^+$ serous ovarian tumors in all hESCT injected with $ALDH^+$ ovarian cancer cells (Fig 5A and C). Strong p53 stain was not identified in hESCT alone or from hESCT injected with $ALDH^+$ cells from a benign fibroadenoma (data not shown). $ALDH^+$ ovarian cancer cells injected subcutaneously in the flank showed no growth during this time period. Finally we repeated this experiment, directly comparing the growth within hESCT of $ALDH^+$ and $ALDH^-$ cells within from 3 patients. hESCT injected with $ALDH^+$ CSC demonstrated much more rapid growth than hESCT injected with paired $ALDH^-$ cells, indicating likely CSC engraftment in hESCT (Fig 5B). Once again, p53 IHC of resected hESCT-$ALDH^+$ CSC tumors demonstrated stain in regions consistent with papillary serous tumor growth (Fig 5C). No p53 stain was noted in any of the hESCT-$ALDH^-$cell tumors, thus the ‘tumors’ that grow in the $ALDH^-$ hESCT represent benign teratoma growth. These data demonstrate that primary ovarian CSC engraft in the human hESCT microenvironment more efficiently than in murine subcutaneous tissue.

DISCUSSION

These data demonstrate that the hESCT-cancer model expresses bona fide *human tumor vessels*. These vessels express not only the expected human vascular markers such as CD31 but also tumor type-specific tumor vascular markers (TVMs) such as EGFL6 and TEM7. A central rationale for the development of such model system is for the testing of novel vascular-targeted therapeutics. A major challenge for developing antibody-based therapies targeting tumor vessels has been the lack of an animal model with a human tumor microenvironment and human vessels; antibodies targeting human antigens cannot be tested in traditional animal tumor models unless the antibodies happen to cross-react between species. The model advanced here addresses this issue and thus allows screening of potential immunotherapeutics targeting human vascular antigens. Similarly, this model can also be used to test the in vivo binding activity of vascular-targeted peptides (23, 31, 32).

The generation of large numbers of human tumor vessels in this model required the addition of VE-$Cadherin^+$ human tumor vascular cells. Interestingly, the addition of only 5,000 vascular cells led to nearly 80% human tumor vessels, ~70% of which were not derived from hESC, suggesting that the human VE-$Cadherin^+$ cells are proliferating within the hESCT. Importantly, the human vessels in this model persisted throughout the period of tumor growth (4–12 weeks after cancer cell injection).

The need to add freshly isolated human tumor vascular cells could limit the widespread utility of this model. However, a significant number of human vessels (~40%) could still be generated in the absence of human tumor vascular cells with the addition of irradiated mouse embryonic fibroblasts. It is possible that the addition of other pro-angiogenic cells such mesenchymal stem cells (33) or tumor-associated myeloid cells (34) could further increase the percentage of human vessels. One limitation for therapeutic testing with this model, as with other murine tumor models of human vasculature, is that tumors are still ultimately dependent on the murine vasculature for blood flow. Therefore, even with the complete therapeutic elimination of the human tumor vessels, tumors regions supplied by the murine tumor vasculature will continue to grow.

While we used our model to confirm anti-vascular therapeutics, it can also potentially be used to test vascular imaging agents specifically targeting human vessels. This model allows testing the sensitivity of these compounds to detect tumor vasculature of 'early stage' tumors. We believe that this murine model offers a means to investigate the basic biology of human TVMs in vivo. Specifically, the mechanism of tumor specific TVM induction could be addressed, due to the power to independently modulate the expression patterns of the hESC and the cancer cells themselves. This may be particularly relevant given that we observed differential induction of some tumor-specific TVMs by breast versus ovarian cancer cell lines.

Finally, the above data demonstrate that this model permits direct engraftment of primary human CSC in a manner more efficient than subcutaneous injections. This expands upon and is consistent with previous reports demonstrating improved growth of primary ovarian cell lines within hESCT as compared to tumor flanks (21, 22). Our previous studies using flank models for the engraftment of $ALDH^+$ ovarian CSC demonstrated engraftment rates of ~20%, and tumor growth required 6–12 months (26). Using the hESCT model, we found 100% engraftment from as few as 700 $ALDH^+$ primary human CSC within 4–12 weeks of tumor cell injection within the hESCT. This model therefore represents a new tool to enhance the efficiency of the study of primary human CSC. This model could potentially be further improved with the addition of cancer associated mesenchymal stem cells (35). These findings emphasize the importance of the interplay between the tumor and the surrounding microenvironment and will allow a dissection of the signals within the tumor microenvironment that support cancer stem cell survival, proliferation, and differentiation.

CONCLUSIONS

We have confirmed the expression of human TVMs in a murine tumor model with robust human tumor vasculature. Importantly many of these TVMs appear to be tumor type specific, indicating a tumor niche dependent induction of these TVMs. This model is a useful tool to study therapeutics targeting human tumor vessels. In addition, this model with its unique human tumor microenvironment allowed 100% engraftment of primary human CSC. The hESCT system will allow deeper probing of the role of the microenvironment dependent induction of TVMs, their role in tumor biology, and interactions in the tumor vascular/cancer stem cell niche.

Supplementary Material

Refer to Web version on PubMed Central for supplementary material.

Acknowledgments

We thank the members of the UMCCC Flow Cytometry and Histology Cores for assistance in the experiments in this manuscript.

Grant Support

This work was initiated with support of the Damon Runyon Cancer Research Foundation and completed with the support of the NIH New Investigator Innovator Directors Award grant #00440377. Breast cancer studies were supported by the University of Michigan Cancer Center Support Grant CA046592. D. Burgos-Ojeda was supported by the NIH Cellular and Molecular Biology Training Grant T32-GM07315. K. Skorecki and M. Tzukerman receive research grant support from the Israel Science Foundation, and the Daniel Soref and Richard Satell Foundations at the American Technion Society.

References

1. St Croix B, Rago C, Velculescu V, Traverso G, Romans KE, Montgomery E, et al. Genes expressed in human tumor endothelium. Science. 2000; 289:1197–202. [PubMed: 10947988]
2. Pasqualini R, Moeller BJ, Arap W. Leveraging molecular heterogeneity of the vascular endothelium for targeted drug delivery and imaging. Semin Thromb Hemost. 2010; 36:343–51. [PubMed: 20490984]
3. Zhong X, Ran YL, Lou JN, Hu D, Yu L, Zhang YS, et al. Construction of human liver cancer vascular endothelium cDNA expression library and screening of the endothelium-associated antigen genes. World J Gastroenterol. 2004; 10:1402–8. [PubMed: 15133843]
4. Allinen M, Beroukhim R, Cai L, Brennan C, Lahti-Domenici J, Huang H, et al. Molecular characterization of the tumor microenvironment in breast cancer.[see comment]. Cancer Cell. 2004; 6:17–32. [PubMed: 15261139]
5. Bhati R, Patterson C, Livasy CA, Fan C, Ketelsen D, Hu Z, et al. Molecular Characterization of Human Breast Tumor Vascular Cells. Am J Pathol. 2008; 172:1381–90. [PubMed: 18403594]
6. Seaman S, Stevens J, Yang MY, Logsdon D, Graff-Cherry C, St Croix B. Genes that distinguish physiological and pathological angiogenesis. Cancer Cell. 2007; 11:539–54. [PubMed: 17560335]
7. Buckanovich RJ, Sasaroli D, O'Brien-Jenkins A, Botbyl J, Hammond R, Katsaros D, et al. Tumor Vascular Proteins as Biomarkers in Ovarian Cancer. Journal of Clinical Oncology. 2007; 25:852–61. [PubMed: 17327606]
8. Lu C, Bonome T, Li Y, Kamat AA, Han LY, Schmandt R, et al. Gene alterations identified by expression profiling in tumor-associated endothelial cells from invasive ovarian carcinoma. Cancer Res. 2007; 67:1757–68. [PubMed: 17308118]
9. Madden SL, Cook BP, Nacht M, Weber WD, Callahan MR, Jiang Y, et al. Vascular gene expression in nonneoplastic and malignant brain. Am J Pathol. 2004; 165:601–8. [PubMed: 15277233]
10. Priebe A, Buckanovich RJ. Ovarian tumor vasculature as a source of biomarkers for diagnosis and therapy. Expert Rev Obstet Gynecol. 2007; 3:65–72.
11. Nanda A, St Croix B. Tumor endothelial markers: new targets for cancer therapy. Current Opinion in Oncology. 2004; 16:44–9. [PubMed: 14685092]
12. Burgos-Ojeda D, Rueda BR, Buckanovich RJ. Ovarian cancer stem cell markers: prognostic and therapeutic implications. Cancer Lett. 2012; 322:1–7. [PubMed: 22334034]
13. Halin C, Rondini S, Nilsson F, Berndt A, Kosmehl H, Zardi L, et al. Enhancement of the anti-tumor activity of interleukin-12 by targeted delivery to neovasculature. Nat Biotechnol. 2002; 20:264–9. [PubMed: 11875427]
14. Cryan LM, Rogers MS. Targeting the anthrax receptors, TEM-8 and CMG-2, for antiangiogenic therapy. Front Biosci. 2011; 16:1574–88. [PubMed: 21196249]
15. Chaudhary A, Hilton MB, Seaman S, Haines DC, Stevenson S, Lemotte PK, et al. TEM8/ANTXR1 blockade inhibits pathological angiogenesis and potentiates tumoricidal responses against multiple cancer types. Cancer Cell. 2012; 21:212–26. [PubMed: 22340594]
16. Milowsky MI, Nanus DM, Kostakoglu L, Sheehan CE, Vallabhajosula S, Goldsmith SJ, et al. Vascular targeted therapy with anti-prostate-specific membrane antigen monoclonal antibody J591 in advanced solid tumors. J Clin Oncol. 2007; 25:540–7. [PubMed: 17290063]
17. Sanz L, Cuesta AM, Salas C, Corbacho C, Bellas C, Alvarez-Vallina L. Differential transplantability of human endothelial cells in colorectal cancer and renal cell carcinoma primary xenografts. Lab Invest. 2009; 89:91–7. [PubMed: 19002108]
18. Bussolati B, Grange C, Tei L, Deregibus MC, Ercolani M, Aime S, et al. Targeting of human renal tumor-derived endothelial cells with peptides obtained by phage display. J Mol Med. 2007; 85:897–906. [PubMed: 17384922]
19. Nor JE, Peters MC, Christensen JB, Sutorik MM, Linn S, Khan MK, et al. Engineering and characterization of functional human microvessels in immunodeficient mice. Laboratory Investigation. 2001; 81:453–63. [PubMed: 11304564]
20. Calabrese C, Poppleton H, Kocak M, Hogg TL, Fuller C, Hamner B, et al. A perivascular niche for brain tumor stem cells. Cancer Cell. 2007; 11:69–82. [PubMed: 17222791]

21. Tzukerman M, Rosenberg T, Reiter I, Ben-Eliezer S, Denkberg G, Coleman R, et al. The influence of a human embryonic stem cell-derived microenvironment on targeting of human solid tumor xenografts. Cancer Res. 2006; 66:3792–801. [PubMed: 16585206]
22. Tzukerman M, Rosenberg T, Ravel Y, Reiter I, Coleman R, Skorecki K. An experimental platform for studying growth and invasiveness of tumor cells within teratomas derived from human embryonic stem cells. Proc Natl Acad Sci U S A. 2003; 100:13507–12. [PubMed: 14573705]
23. Winer I, Wang S, Lee YE, Fan W, Gong Y, Burgos-Ojeda D, et al. F3-targeted cisplatin-hydrogel nanoparticles as an effective therapeutic that targets both murine and human ovarian tumor endothelial cells in vivo. Cancer Res. 2010; 70:8674–83. [PubMed: 20959470]
24. Wu R, Hu TC, Rehemtulla A, Fearon ER, Cho KR. Preclinical testing of PI3K/AKT/mTOR signaling inhibitors in a mouse model of ovarian endometrioid adenocarcinoma. Clin Cancer Res. 2011; 17:7359–72. [PubMed: 21903772]
25. Wu R, Hendrix-Lucas N, Kuick R, Zhai Y, Schwartz DR, Akyol A, et al. Mouse model of human ovarian endometrioid adenocarcinoma based on somatic defects in the Wnt/beta-catenin and PI3K/Pten signaling pathways. Cancer Cell. 2007; 11:321–33. [PubMed: 17418409]
26. Silva IA, Bai S, McLean K, Yang K, Griffith K, Thomas D, et al. Aldehyde dehydrogenase in combination with CD133 defines angiogenic ovarian cancer stem cells that portend poor patient survival. Cancer Res. 2011; 71:3991–4001. [PubMed: 21498635]
27. Pulaski HL, Spahlinger G, Silva IA, McLean K, Kueck AS, Reynolds RK, et al. Identifying alemtuzumab as an anti-myeloid cell antiangiogenic therapy for the treatment of ovarian cancer. J Transl Med. 2009; 7:49. [PubMed: 19545375]
28. Tzukerman M, Skorecki KL. A novel experimental platform for investigating cancer growth and anti-cancer therapy in a human tissue microenvironment derived from human embryonic stem cells. Methods Mol Biol. 2006; 331:329–46. [PubMed: 16881525]
29. Tzukerman M, Skorecki K. A novel experimental platform for investigating tumorigenesis and anti-cancer therapy in a human microenvironment derived from embryonic stem cells. Discov Med. 2003; 3:51–4. [PubMed: 20705041]
30. Theriault C, Pinard M, Comamala M, Migneault M, Beaudin J, Matte I, et al. MUC16 (CA125) regulates epithelial ovarian cancer cell growth, tumorigenesis and metastasis. Gynecol Oncol. 2011; 121:434–43. [PubMed: 21421261]
31. Kolonin MG, Sun J, Do KA, Vidal CI, Ji Y, Baggerly KA, et al. Synchronous selection of homing peptides for multiple tissues by in vivo phage display. FASEB J. 2006; 20:979–81. [PubMed: 16581960]
32. Hajitou A, Pasqualini R, Arap W. Vascular targeting: recent advances and therapeutic perspectives. Trends Cardiovasc Med. 2006; 16:80–8. [PubMed: 16546688]
33. Spaeth EL, Dembinski JL, Sasser AK, Watson K, Klopp A, Hall B, et al. Mesenchymal stem cell transition to tumor-associated fibroblasts contributes to fibrovascular network expansion and tumor progression. PLoS One. 2009; 4:e4992. [PubMed: 19352430]
34. McLean K, Buckanovich RJ. Myeloid cells functioning in tumor vascularization as a novel therapeutic target. Transl Res. 2008; 151:59–67. [PubMed: 18201673]
35. McLean K, Gong Y, Choi Y, Deng N, Yang K, Bai S, et al. Human ovarian carcinoma-associated mesenchymal stem cells regulate cancer stem cells and tumorigenesis via altered BMP production. J Clin Invest. 2011; 121:3206–19. [PubMed: 21737876]

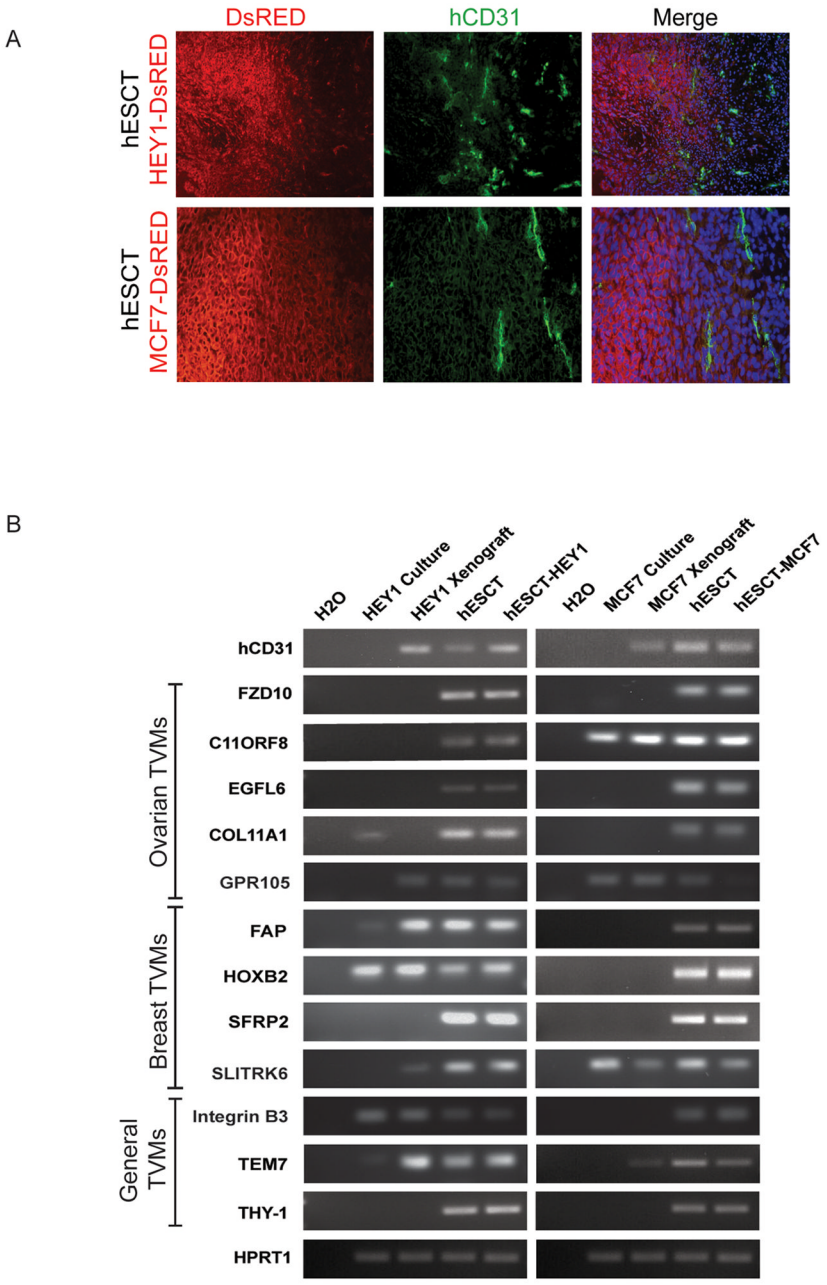

Figure 1. Validation of human vasculature in the hESCT-cancer model

(A) Co-IF demonstrating the presence of hCD31^{+} (green) vascular structures in a peritumoral location with DsRed cancer cells. **(B)** RT-PCR of TVMs expression in the indicated cancer cell line cultures, tumor cell line xenografts, hESCT, and hESCT-cancer models.

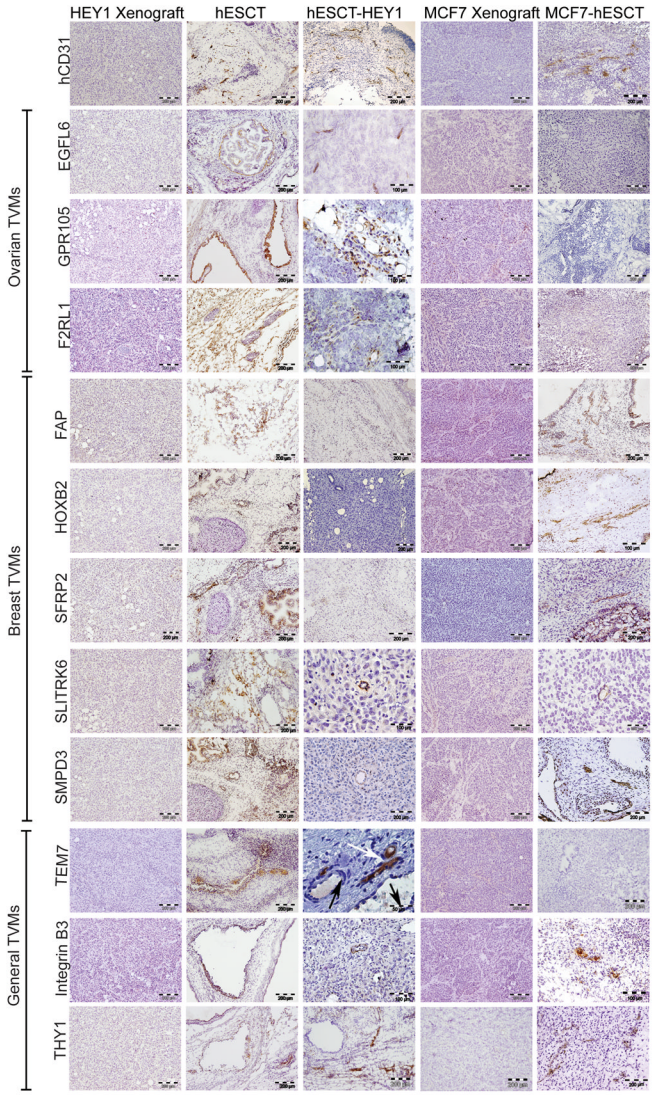

Figure 2. TVM expression in the vasculature is influenced by the cancer cells

IHC localization of ovarian cancer specific TVMs, breast cancer specific TVMs and non-tumor specific general TVMs in the indicated tumors. While TVMs are expressed in various developmental tissues of the hESCT, vascular expression of TVMs is primarily seen only in the presence of cancer cells in a tumor type specific manner. n= 4 animals/group in two experiments. Black arrow indicates vessel containing red blood cells.

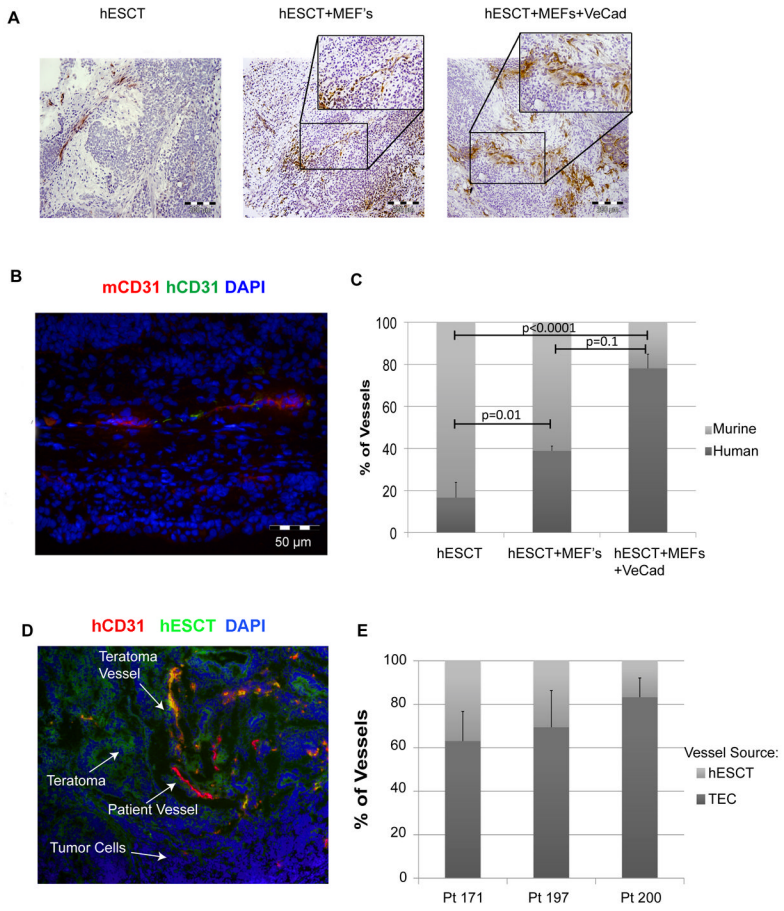

Figure 3. Enhancing the number of human vessels in the hESCT-cancer model

(A) IHC of hCD31 in hESCT-HEY1, hESCT-HEY1-MEFs, hESCT-HEY1+MEFs+VE-Cadherin^{+}. **(B)** IF showing inter-connection of mouse and human vessels. **(C)** Quantification of mouse and human vessels in the hESCT-cancer model alone, with MEFs, or with MEFS and VE-Cadherin^{+} cells. p values are indicated with error bars representing standard deviations. n=4 animal/group. **(D)** Co-IF demonstrating hCD31 stain (red) in both hESCT-GFP cells (green) resulting in yellow hESC derived vessels, and non-GFP cells originating from VE-Cadherin isolated patient tumor endothelial cells (patient vessels). **(E)** Quantification of the percentage of hESCT derived and patient tumor endothelial cell (TEC) derived vessels.

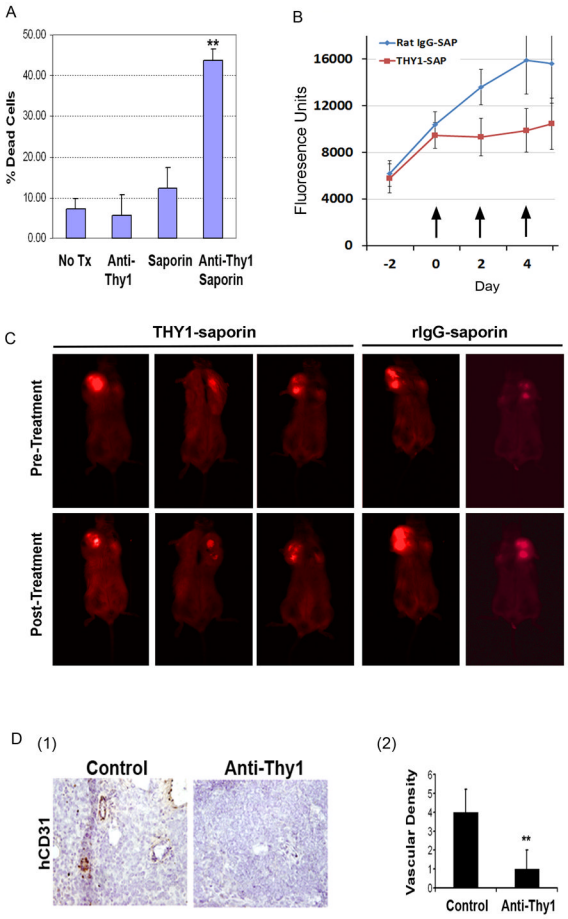

Figure 4. Testing Anti-TVM Therapeutics in the hESCT-HEY1 ovarian tumor model

(A) Quantification of cellular death of THY1 expressing MSC treated with anti-THY1-saporin immunotoxin and controls. **(B)** Biofluorescence of hESCT-HEY1 DsRed ovarian tumor before and after two treatments with anti-THY1-saporin immunotoxin arrows indicated time of treatment. **(C)** Biofluorescent images of hESCT-HEY1 DsRED tumors before and after treatment with the indicated immunotoxins. **(D)** IHC images (1) and (2) quantification of human tumor vessels in control and Anti-THY1-saporin treated tumors. Error bars represent standard deviations.

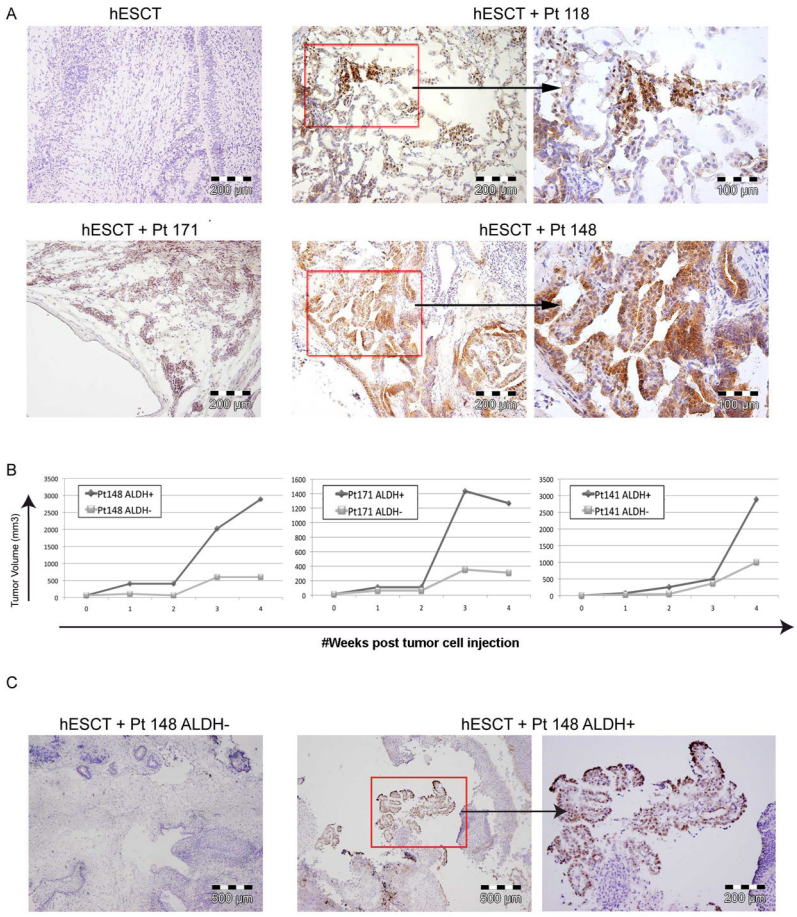

Figure 5. Growth of primary ovarian CSCs using the hESCT model

(A) p53 IHC demonstrating ovarian cancer cells initiated by $ALDH^+$ CSC injected within the hESCT. hESCT alone and $ALDH^+$ cells from a patient with a benign fibroadenoma demonstrated no growth. (B) hESCT-ovarian tumor volumes from hESCT injected with 10,000 $ALDH^+$ or $ALDH^-$ ovarian cancer cells from three patients. (C) p53 IHC of hESCT injected with $ALDH^-$ cancer cells and $ALDH^+$ cancer cells demonstrating $p53^+$ papillary serous tumor growth from $ALDH^+$ tumor only.